

# Fiber optic method for health assessment of pipelines subjected to earthquake-induced ground movement

Branko Glisic and Yao Yao

Structural Health Monitoring

0(0) 1–16

© The Author(s) 2012

Reprints and permissions:

sagepub.co.uk/journalsPermissions.nav

DOI: 10.1177/1475921712455683

shm.sagepub.com



## Abstract

Natural disasters, in particular earthquakes, can cause damage to pipelines with disastrous humanitarian, social, economic, and ecologic consequences. Thus, real-time, automatic, or on-demand assessment of damage to pipelines after the earthquake is essential for early emergency response, efficient preparation of rescue plans, and mitigation of these disastrous consequences. This article presents the development of a method for buried pipelines health assessment based on distributed fiber optic sensors, which are sensitive to strain at every point along their lengths. The sensors are both bonded to pipeline and embedded in the soil, in the proximity of the pipeline. The research includes determination of sensor topology, identification of required sensor properties, selection of sensors, development of installation procedures, implementation, and validation. The validation of the method was made through a large-scale testing: a 13-m-long real-size concrete segmented pipeline was assembled in a large test basin filled with soil and was tested under simulated permanent ground displacement. The basin consisted of two parts: the movable north part and the fixed south part. The movable north part of the test basin was attached to four hydraulic actuators, which were used to apply controlled displacement of the basin, and it induced damage to the pipeline by crushing the joints between adjacent pipeline segments. As a part of validation, the results obtained from distributed sensors were compared with resistive strain gauges. Two validation tests were performed: the first in 2010 and the second in 2011. The method is presented in detail, and the most significant results of both tests are analyzed, compared, and discussed. The validation tests confirmed the capacity of the method to reliably detect and localize the damage on pipeline and the displacement in the soil.

## Keywords

Damage detection and localization, distributed fiber optic sensors, structural health monitoring of pipelines, earthquake-induced permanent ground displacement, large-scale validation testing

## Introduction

Real-time, automatic, or on-demand assessment of damage to pipelines after the earthquake is essential for early emergency response, efficient preparation of rescue plans, and mitigation of the disastrous consequences. Assessment is particularly challenging for buried pipelines since they are under the soil. Earthquake-induced damage for pipelines is in general classified as being generated by transient ground deformation (TGD) or permanent ground deformation (PGD).<sup>1</sup> Historical records are concordant with a widely accepted opinion that the most serious cases of earthquake-induced damage to pipelines were generated by strong ground motion or site failure,<sup>2</sup> and that is why this research focus on the damage generated by PGD. The distribution of PGD depends on several

factors, such as intensity and duration of earthquakes, site grade, soil type, type of pipeline, and the location of the water table.<sup>3</sup>

Existing technologies employed for inspection of buried pipelines are mainly based on the use of devices that can be inserted in the interior of the pipeline. These devices may contain various types of sensors, typically depending on the type of the pipeline. The most common device used for inspection of metallic pipelines is

---

Department of Civil and Environmental Engineering, Princeton University, Princeton, NJ 08544, USA

### Corresponding author:

Branko Glisic, Department of Civil and Environmental Engineering, Princeton University, E330 EQuad, Princeton, NJ 08544, USA.

Email: bglisic@princeton.edu

the so-called pig.<sup>4</sup> It is a small package containing mostly two types of sensing transducers: remote field eddy current and ultrasonic transducers.<sup>5</sup> For concrete pipelines, cameras are either placed on a robot and moved through the pipeline using the robotic system<sup>6</sup> or simply installed at a manhole access point. Besides the use of a camera, ultrasonic systems can also be used when the internal area of a pipeline is accessible.<sup>7</sup> The acoustic and ultrasonic transducers can also be installed on the surface of the pipeline. Piezoelectric elements can be mounted on the walls of the pipeline and they can introduce guided elastic waves, called Lamb waves, into the walls of pipeline. However, Lamb waves are of limited application for concrete pipelines due to their high attenuation.<sup>8</sup> Remote sensing technologies for monitoring concrete pipelines deployed above the surface are infrared thermography systems (ITS) that capture thermal images of soil altered by leaks due to the rupture of pipeline<sup>9</sup> and ground penetrating radar (GPR) that captures reflections from boundaries of two different dielectrics and detects damage as alterations. Both technologies are challenged by reliable image interpretation. Although several existing technologies are employed for assessment of pipeline health condition, none of them is entirely suitable for the real-time automated operation. In general, they require manual operation and data analysis, which adds subjectivity to the process. Recent researches propose novel approaches to the assessment of the pipeline health condition. They are based on the self-detection capacity of cementitious materials, that is, on the damage-induced changes in their electrical properties<sup>10</sup> and acoustic properties<sup>11</sup> combined with the use of wireless technologies.<sup>12</sup> These researches are ongoing and have a very promising potential for applications on buried structures.<sup>13</sup>

Strain monitoring based on discrete<sup>14</sup> and distributed<sup>15</sup> fiber optic sensing was introduced in the recent years. The discrete sensors feature better measurement properties (higher resolution, accuracy, and frequency of reading), but they must be sparsely spaced and either provide severely insufficient spatial resolution for early damage detection or rely on complex algorithms that degrade specificity against environmental and variable load conditions. Thus, they are rather suitable for a local monitoring of critical pipeline sections than for the global pipeline integrity monitoring. The distributed sensors can overcome the spatial resolution and specificity challenges related to discrete sensors-based monitoring.

A novel method for real-time, automatic, or on-demand assessment of health condition of buried pipelines after the earthquake is developed. The method is based on the use of distributed fiber optic sensing technology and it focused on concrete segmented pipelines,

but it can be extended to steel continuous pipelines. Besides the assessment of damage, the method can be used for long-term structural health monitoring and operational monitoring, which will serve as an important input for lifetime maintenance activities. The central part of the project, validation testing, was performed at Network for Earthquake Engineering Simulation (NEES) Lifeline Experimental and Testing Facilities at Cornell University. In a broader scope, the validation testing involved participation of several other universities: University of Michigan, Ann Arbor, Michigan; Virginia Tech; Merrimack College; and Purdue University. Strain gauge measurements collected by University of Michigan were compared with results obtained from fiber optic sensors (FOS) in order to better understand their functioning. The method was validated through two tests, and the results are presented and discussed in this article.

## Distributed sensing

The method researched and developed in this project is based on the use of distributed fiber optic strain monitoring system. Strain sensing is proposed, since the PGD actually strains the pipeline, and the distributed technology is proposed taking into consideration particularly large lengths of the pipelines and the uncertainty of the location in which the damage can occur.

Distributed sensor (or sensing cable) can be represented by a single cable, which is sensitive at every point along its length. Hence, one distributed sensor can replace thousands of discrete sensors. Moreover, it requires single connection cable to transmit the information to the reading unit, instead of a large number of connecting cables required in the case of wired discrete sensors. Finally, distributed sensors are less difficult and more economic to install and operate. An illustrative comparison between pipelines equipped with distributed and discrete sensors is shown in Figure 1.

There are three main principles for distributed sensing using FOS: Rayleigh scattering,<sup>16</sup> Raman scattering,<sup>17</sup> and Brillouin scattering.<sup>18</sup> Stimulated<sup>19</sup> Brillouin scattering has been selected because it is least sensitive to cumulated optical losses and it allows for monitoring of exceptionally large lengths.<sup>20,21</sup> The performance and the cost of the distributed sensors depend on the sensor packaging. The packaging that provides with a very good strain transfer from the structure to the measurement optical fiber, that is, with high measurement accuracy, is expensive. In addition, this packaging is mechanically less robust, which makes them challenging to handle and install. In contrary, mechanically robust packaging is less expensive, but as the strain transfer is less good, it provides with less accurate measurements.

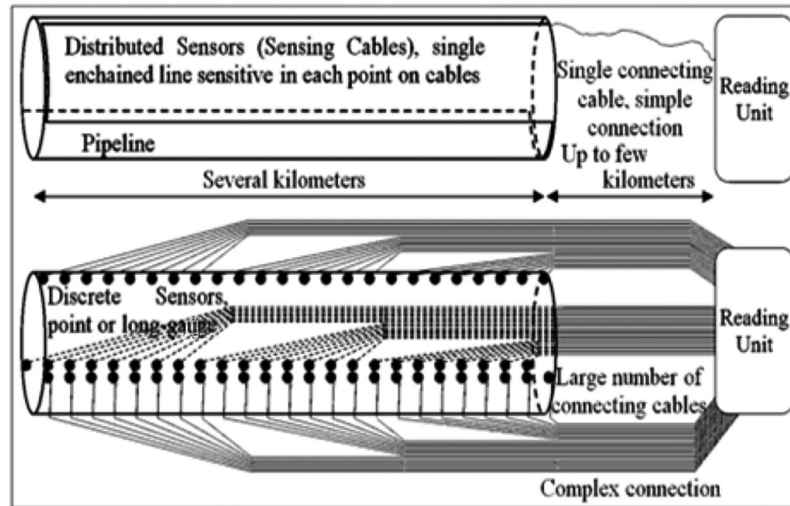


**Figure 1.** Distributed versus discrete monitoring (schematic drawing, does not refer to real case).

Three types of sensors were selected for tests and they are briefly presented here.

“Tape” sensor (see Figure 2) contains one measurement optical fiber embedded in a thermoplastic composite tape.<sup>21</sup> It features high strain transfer and high accuracy (error limits estimated to approximately  $\pm 20 \mu\epsilon$ , depending on the quality of installation), but its cost is elevated, and it needs cautions when handling and installing, as it features low mechanical robustness. “Profile” sensor (see also Figure 2) contains two measurement and two loose optical fibers embedded in a polyethylene profile.<sup>21</sup> It features moderate strain transfer (i.e. moderate accuracy, estimated error limits approximately ranged between  $\pm 20$  and  $\pm 50 \mu\epsilon$ , depending on the quality of installation), moderate

cost, and it is easy to handle and install as it is mechanically robust.

“Cord” sensor (see Figure 3) contains two measurement fibers and two loose fibers. Measurement fibers are “squeezed” between the inner and the outer plastic tube, and the strain transfer is performed by friction; this provides with a weak strain transfer and a very low accuracy (error limits by absolute value are much larger than  $50 \mu\epsilon$ ), as the fibers can slide between the tubes. However, low cost, extended range of measurements, and very high mechanical robustness make this sensor very attractive for applications in pipeline monitoring.

### Sensor topology

The capability of distributed FOS to reliably detect and localize damage depends on their topology, and more specifically, on their total number and position on the pipeline and in the soil. Topology of sensors depends on the expected pipeline failure mode, which depends on the pipeline type.

A segmented gravity pipeline was available for the method validation test, and the focus in sensor topology determination was on this type of pipeline. Based on the experience in previous tests, the failure of segmented pipeline occurs mainly by crushing of bell-and-spigot joints.<sup>13</sup> An example of failure caused by crushing of bell-and-spigot joint is shown in Figure 4.

Parallel topology<sup>22</sup> is selected as the best feasible configuration for both sensors installed on the pipeline and sensors embedded in the soil. For the installation on the pipeline, the parallel topology consists of at least three parallel sensors installed (glued) along the pipeline as shown in Figure 1. Minimum three sensors are

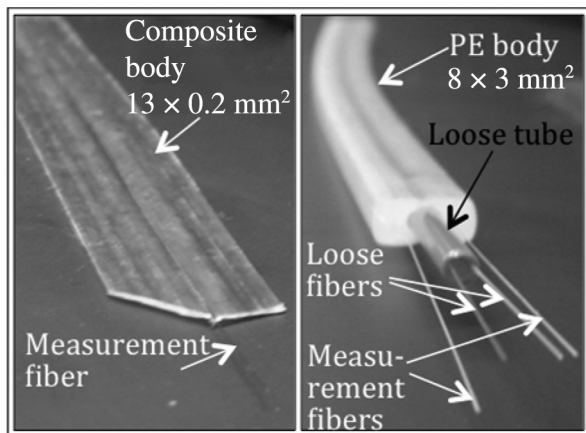


**Figure 2.** Views of Tape sensor (left) and Profile sensor (right). PE: polyethylene.

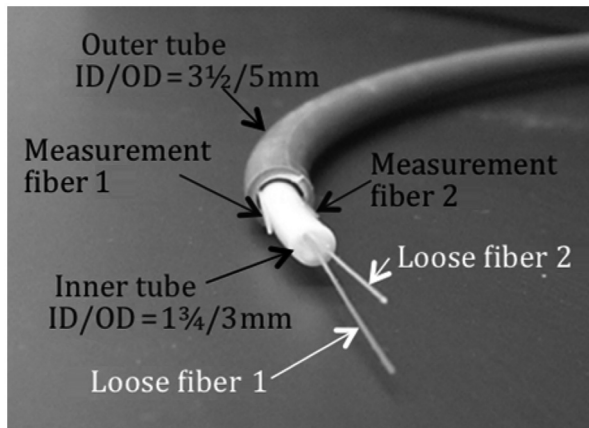


**Figure 3.** View of Cord sensor (sensing cable).

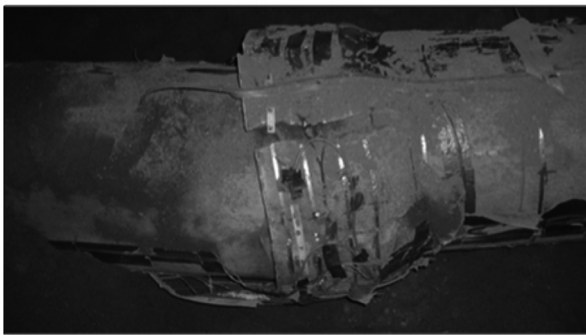


**Figure 4.** Crushing of bell-and-spigot joint for a segmented pipeline.

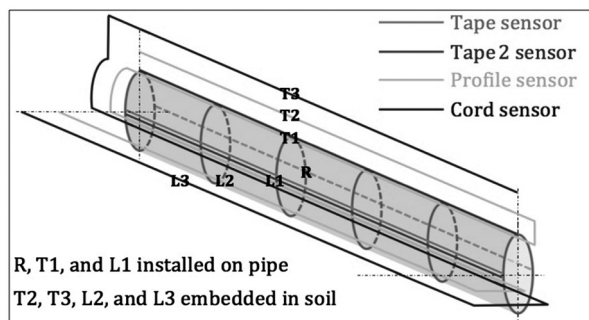


**Figure 5.** Physical layout of sensors in the first test; Cord and Profile sensors were in the form of serpentine.

needed to fully describe spatial deformation of the pipeline,<sup>22</sup> that is, axial deformation (elongation or contraction) and bending in horizontal and vertical planes, and to provide for sufficient spatial sensitivity to damage. Information on spatial deformation of the pipeline serves as an early warning about potentially

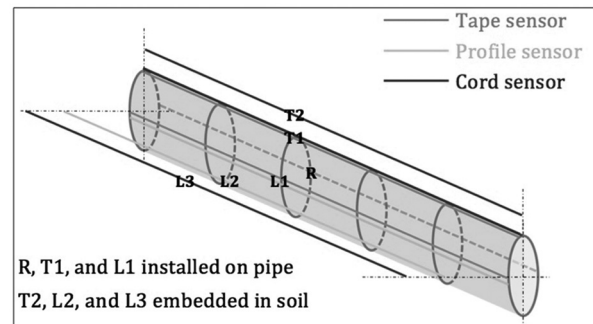


**Figure 6.** Physical layout of sensors in the second test; all sensors installed as “individual lines.”

high stresses in the pipeline. High spatial sensitivity to damage is needed, as the location and direction of the permanent ground displacement (PGD) are not known before the earthquake.

For the sensors installed in the soil, the parallel topology consists of at least one sensor installed parallel to the pipeline. The sensor in the soil cannot provide with spatial deformation or damage of the pipeline, but it can detect and localize the movements in the soil that can potentially imperil the pipeline, and it can point to endangered locations. Although this approach is not direct, it can be very efficient if proven to be reliable, since the embedding in the soil is significantly simpler and faster than bonding sensors onto the pipeline.

The parallel topology was tested and its suitability for segmented pipeline monitoring was confirmed by the test. Positions of the sensors as tested in the two tests are given in Figures 5 and 6, respectively (see also Figure 14). Long Cord sensing cable (more than three times longer than the tested pipeline specimen) used in the first test was installed in the form of a serpentine covering three locations: T3, L1, and L3 (see Figure 5). Similarly, a long Profile sensing cable (more than four times longer than the tested pipeline specimen) was installed in the form of a serpentine covering four locations: T2, T1, L1, and L2 (see Figure 5). All the other sensors in the first test (Cord sensor at location T1 and all Tape sensors, see Figure 5) as well as all the sensors in the second test (see Figure 6) had approximately the same length as the tested specimens and were installed as “individual lines” (i.e. not in the form of serpentes). The serpentine form of Cord and Profile sensors influenced results of the first test as discussed in section “Data analysis.”

## Installation procedure

In order to guarantee the strain transfer from the pipeline to the sensors, it was decided to glue the sensors over the entire length of the pipeline. Clamping the



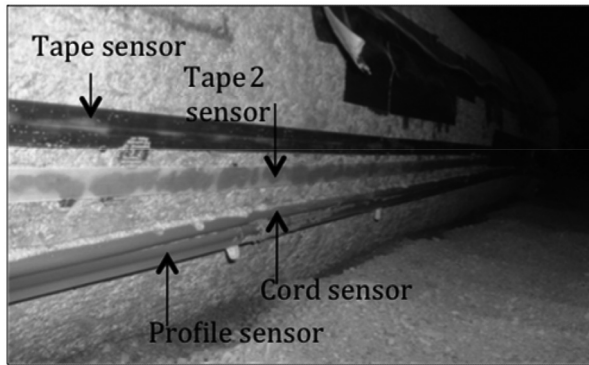


**Figure 7.** Sensors installed on the pipeline (first test).



**Figure 8.** Gluing of sensors, detail at joint (second test).

sensor would be time-consuming and expensive as the full circumference of the pipeline has to be accessible at large number of closely spaced points. The adhesive was carefully selected for each type of sensor in order to match with materials to be bonded. In particular, adhesive should provide not only good adhesion of Tape sensors to the pipeline but also delamination of sensors in the case of cracking of the pipeline in order to prevent damaging of the sensor.<sup>23,24</sup> Finally, since the sensors were bonded over their entire lengths, they were capable of monitoring both elongation and contraction, and there was no need to pre-tension the sensors.

The sensors installed on the pipeline are shown in Figure 7. The gluing of the sensors to the pipeline is shown in Figure 8. After the installation, the sensors were covered by duct tape, which provided with protection during the burying of the pipeline. Identical adhesives were used in the second test. The inspection of the sensors after the test has shown good adhesion of sensors over the body of the pipeline (no delamination)

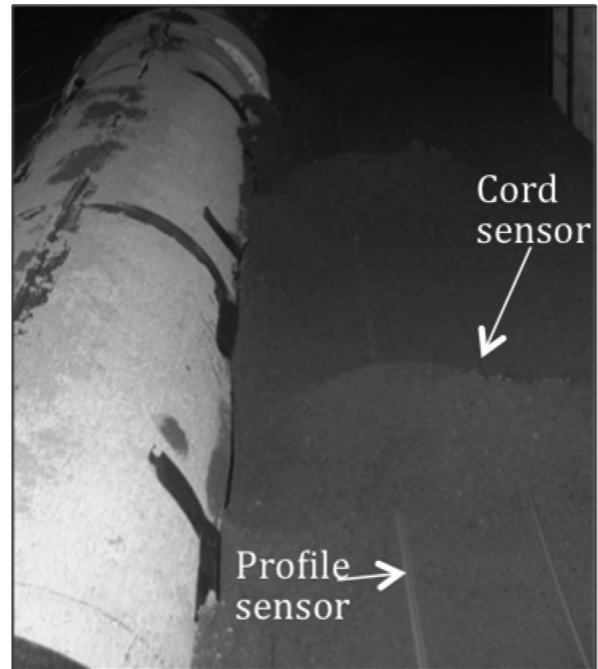


**Figure 9.** Profile and Cord sensors laid and ready for burying (first test).

and, as expected, a delamination of the Tape sensor in cracked zones of the joints, which prevented the damaging of the sensor. The sensors installed in the soil were simply placed at its position and covered with soil, as shown in Figure 9.

Particular issue for the sensor installation is uneven surface of the segmented pipeline. Two issues are related to abrupt changes in the geometry of the pipeline at joints:

1. Sharp changes in geometry can create excessive local bending of the sensor that may result either in rupture of the sensor during the burying or in high attenuation of optical signal; high attenuation of optical signal will make the measurement impossible or unreliable;
2. If small pieces of the sensor are left loose, they might be excessively strained due to compaction of the soil and the measurement of the sensor will be unreliable at these locations; this was confirmed during the second validation test.

In order to protect sensors during the burying and to provide for continuous strain transfer, it was decided for the first test to add small “bridges” made of plastic (polyvinyl chloride (PVC)) at the location of the joints, where the geometry of the pipeline changes abruptly, see Figure 10(a). The first method validation test has shown that this solution was not good: during the

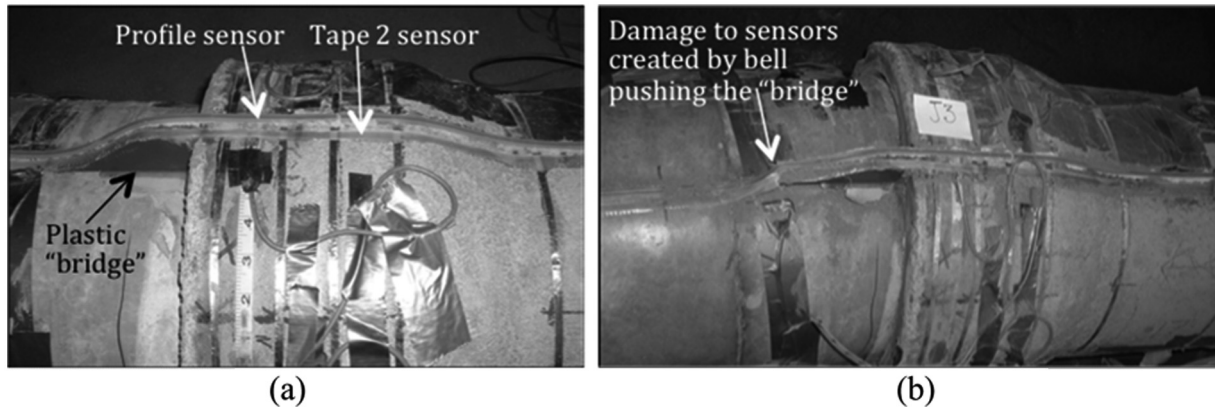


**Figure 10.** (a) Sensor installed over the joint using specially designed “bridge” and (b) damage to sensors generated by bell pushing the “bridge”.



**Figure 11.** (a) First solution: opening in the bell, Profile sensor (up), and Tape sensor (down) and (b) second solution: free sensors over the gap, Tape sensor (closer), and Cord sensor (farther).

crush of the joint, the bell was pushing the “bridges” that resulted in sensor damage, see Figure 10(b). Thus, the installation of sensor over the joints had to be improved. Two solutions for installation over the joints were considered for the second test:

1. As the pipeline segments for the second test were made by research partners from Purdue University, it was possible to modify the bells of the joint, that is, to create openings ( $2.5 \times 2 \text{ cm}^2$ ) in order to pass the sensors through without the bending; once the sensors were in place, they were bonded inside the opening and the holes were filled with the adhesive; this solution was applied for sensors at locations “R” and “L” (see Figures 5 and 6) and it is shown in Figure 11(a);
2. The sensors were left unattached over the gap; during embedding, the space between the sensor and the pipeline body was carefully filled with the soil

in order to give support to the sensor and then the pipeline was completely buried; this solutions is shown in Figure 11(b).

The validation tests fully proved the first solution, while the second solution was not satisfactory. Tape sensor installed in accordance with the second solution, being more fragile, was damaged by soil movements, and Cord sensor provided with ambiguous results. Consequently, only the first procedure is fully recommended, since the validation test confirmed its very good performance.

### Method validation testing

The central part of the project, method validation testing, was performed at The Cornell Large-Scale Lifelines Testing Facility, the NEES site at Cornell University (Cornell NEES Site). The aim of the testing was to

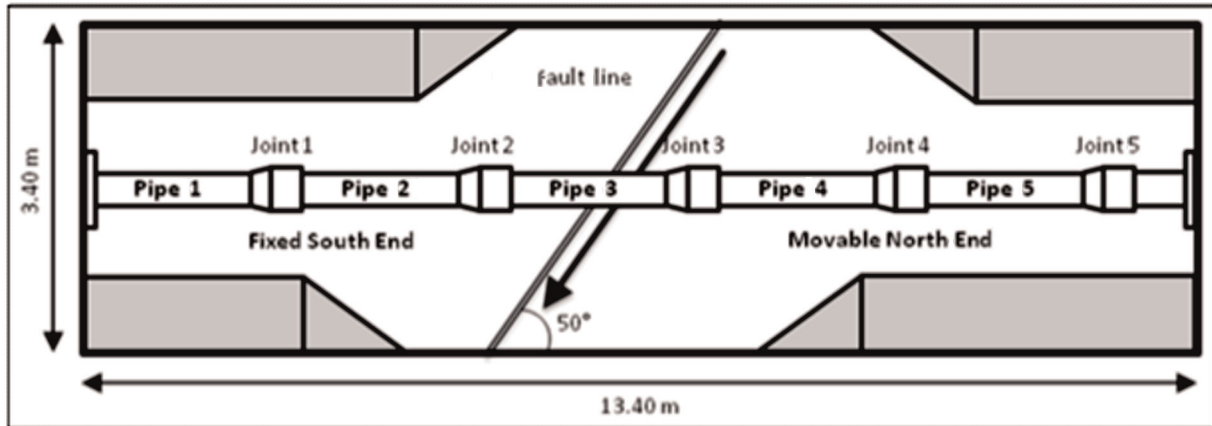


**Figure 12.** Schematic representation of test basin and the pipeline.

validate the researched method for reliable, real-time, automatic, or on-demand assessment of pipelines subject to earthquake-induced PGD. Besides this primary aim, the testing helped evaluate the performance of the deployed distributed sensors in close-to-real conditions. The testing was performed in two phases, the first performed in June 2010 and the second performed in June 2011.

### *Description of the test basin*

The Cornell NEES Site contains a large test basin in which a pipeline can be assembled and tested under simulated PGD. The basin is a 3.40-m-wide, 13.40-m-long, and 2.0-m-deep steel frame box with wooden walls. It consists of two parts: the movable north part and the fixed south part.



**Figure 13.** Hydraulic actuators.

For each test, a segmented concrete pipeline specimen was assembled in the basin and covered with the soil. Schematic view of the pipeline and the basin is given in Figure 12. The movable north part of the test basin was attached to four hydraulic actuators that were anchored in massive concrete counter bearings. During the test, the hydraulic actuators were used for controlled movement of the north part of the basin. The joint between the two parts was designed in a way that a transverse fault oriented  $50^\circ$  relative to the longitudinal length of the basin can be simulated (see Figure 12). The hydraulic actuators are shown in Figure 13.

### *Description of the pipeline specimens*

The pipeline specimen used in the first test consisted of five 2.44-m-long (8 ft) segments (as installed), assembled using 25.4-cm-long (10 in) bell-and-spigot joints sealed by grout. The inner and outer diameters of the pipeline body were 30.5 cm (12 in) and 40.6 cm (16 in), respectively, while the outer diameter at the joint was 50.8 cm (20 in). Short segment of the pipeline was added at the movable (north) extremity in order to provide for mechanical connection with the frontal and rear walls of the basin. It is important to highlight that not all the pipeline segments had the same mechanical properties. The segments 1, 2, 3, and 5 and short extension in the movable part of the basin (see Figure 12) were purchased from the same pipeline manufacturer and had identical mechanical properties. The segment 4 was built of fiber-reinforced concrete by project partner (Purdue University) and had much higher stiffness and resistance (this segment was actually a specimen constructed in the frame of the project partner's research). This segment had also slightly different geometry: the total length of 2.25 m (7.4 ft) and bell length of 30.5 cm (12 in). The influence of higher mechanical properties



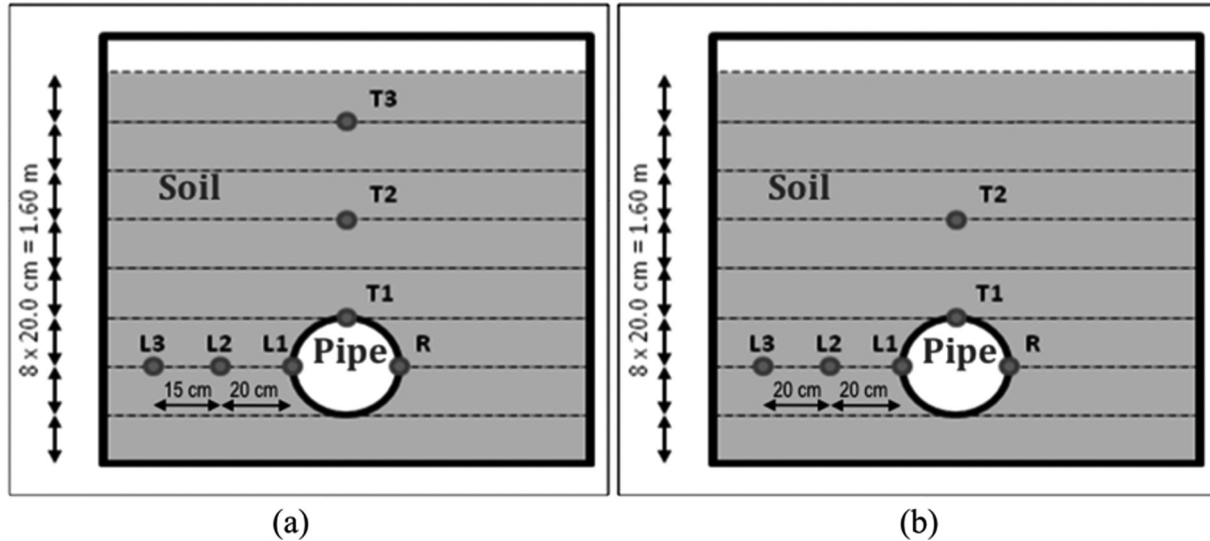


**Figure 14.** Positions of sensors in (a) the first test and in (b) the second test.

of this segment to the results of the test was important as presented in section “Data analysis.”

The pipeline specimen used in the second test consisted of five 2.36-m-long (7 ft 9 in) segments (as installed), assembled using 30.5-cm-long (12 in) bell-and-spigot joints sealed by grout. The other dimensions (the inner and outer diameters of the pipeline body and the outer diameter at the joints) were the same as in the first test. Short segment of the pipeline was added at the movable (north) extremity in order to provide for mechanical connection with the frontal and rear walls of the basin, as in the case of the first test. In the second test, all the pipeline segments had the same mechanical properties. They were built of fiber-reinforced concrete by the project partner (Purdue University). The uniform mechanical properties along the pipeline made the results of the second test different from those obtained in the first test, as presented in section “Data analysis.”

For both tests, the sensors were installed in parallel topology. The positions of the sensors with respect to the cross-section are for both tests given in Figure 14 (see also Figures 5 and 6).

## Data analysis

The data analysis was performed in several steps:

1. Primary data analysis consisted of filtering out the outliers and the noise, interpretation and correlation with load cases and visual inspection of the pipeline after each test (for crack occurrence). Primary data analysis helped identify data patterns characteristic for each performed test and whether

the monitoring system was able to detect and localize the damage.

2. The results obtained from the first step are compared with traditional strain gauges installed along the body of the pipeline specimens (installed and operated by project partner University of Michigan, Ann Arbor, MI); the comparison helped to assess the performance of developed monitoring method.
3. In order to make damage detection and localization automatic, simple, but effective, algorithms based on thresholds “in space” (comparison of strain values along the pipeline) and “in time” (comparison of strain value at each point in time) were applied and their performance verified.

Large amount of data was collected during the tests. The most significant results are presented in this article.

### *Analysis of tape sensor at location L1*

In the first test, the tape sensor at location L1 functioned properly during the first step of the test when relative ground displacement of 2.54 mm (1 in) was applied and damaged the pipeline at the joints 2 and 3 (the joint 2 belongs to pipe segment 2, i.e. it is between pipe segments 2 and 3, etc.). Unfortunately, during the second step, the sensor was broken as a consequence of inappropriate installation procedure (the use of “bridges,” see Figure 10). The results are presented in Figure 15.

The results in the figure represent total noncompensated strain distribution along the pipeline. The temperature compensation was not necessary for damage



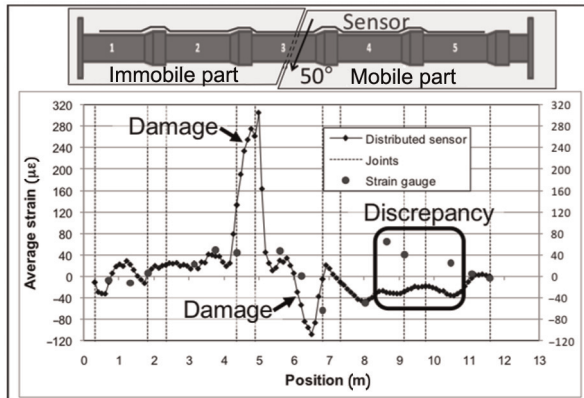


**Figure 15.** Results of test with detected damage (indicated by arrows) in the first test.

Strain gauge values: courtesy of Prof. Lynch group at University of Michigan, Ann Arbor, Michigan.

detection purposes since it only translates vertically the diagram presented in the figure, but this does not influence the interpretation of the data.

Two unusual strain changes were observed, high tension close to joint 2 and high compression close to joint 3. These unusual strain changes actually correspond to locations of actual damage on the pipeline. No damage was detected at the other joints for 25.4 mm (1 in) displacement.

Tape sensor data were compared with strain gauge measurements, see Figure 15. The strain gauge sensors were not installed at the joints (their purpose was not damage detection), but over the body of the pipeline, next to the Tape sensor. The results obtained from two different systems are in a very good correlation, except in three points where some discrepancy is noticed (see Figure 15). This discrepancy is not fully explained, but part of it can certainly be attributed to the short gauge length of strain gauges.

In the second test, Tape sensor at location L1 functioned properly for all the 12 steps of load (12 in of soil displacements). This confirms successful improvement of the installation procedures. However, part of measurements was lost due to high attenuation (optical losses) generated by delamination of measurement fiber from the composite tape during the installation. The zone of the lost data includes the pipeline segments 4 and 5. The data analysis for the rest of the pipeline is shown in Figure 16.

Since the soil shear plane was in the middle of the pipeline, the damage occurred at joints 2 and 3, similar to as in the first test. The results in the diagram represent total noncompensated strain distribution along the pipeline (similar to the analysis performed in the first test).

The damage to pipeline occurred during the seventh step of the load. This was confirmed by high noise observed during the test during the seventh step of the load. The damage was successfully detected and localized by Tape sensor as a high strain at location of damage (pointed with black arrow in Figure 16). Before the damage occurred, the pipeline was subjected to bending and strain distribution and evolution due to bending is observed in the figure. Successful detection of bending is very important, since it can be used as an early indicator of generation of stress in pipeline, which can potentially lead to the damage.

Comparison with strain gauges has shown good agreement between the two technologies. For illustrative purposes, comparison of results for the seventh step of load is shown in Figure 16. The results demonstrated the ability of the system to detect and localize early damage in the form of cracks in close-to-real conditions and in real time.

### *Measurements of Tape sensor at location R and global deformation of the pipeline*

Tape sensor at location R functioned properly only during the first load step (25.4 mm displacement) in the second test and was broken afterward. The reason for sensor malfunction was similar as for the sensor at L1 location: delamination of measurement optical fiber from the tape (and not the installation procedures). Strain distribution at location R measured by the Tape sensor is presented in Figure 17. Comparison with strain gauges is presented in the same figure.

Tape sensor at location R demonstrated similar properties as Tape sensor at location L1: it was able to detect strain change in the pipeline due to bending generated during the first step of the load, and the comparison with strain gauges confirmed very good agreement between the two technologies.

The combination of Tape sensors installed at locations L1 and R reveals global structural behavior of the pipeline under the soil movement:

- Overall axial deformation of the pipeline is contraction;
- The pipeline is bended in the horizontal plane and deflected shape is qualitatively similar to deformed sinusoidal line (see strain distributions in Figures 16 and 17);
- The sensor at location L1 (see Figure 16) measures tension south of shear plane and compression north of shear plane, while the sensor at location R has exactly opposite behavior. This behavior is coherent with deformed shape presented in Figure 17;

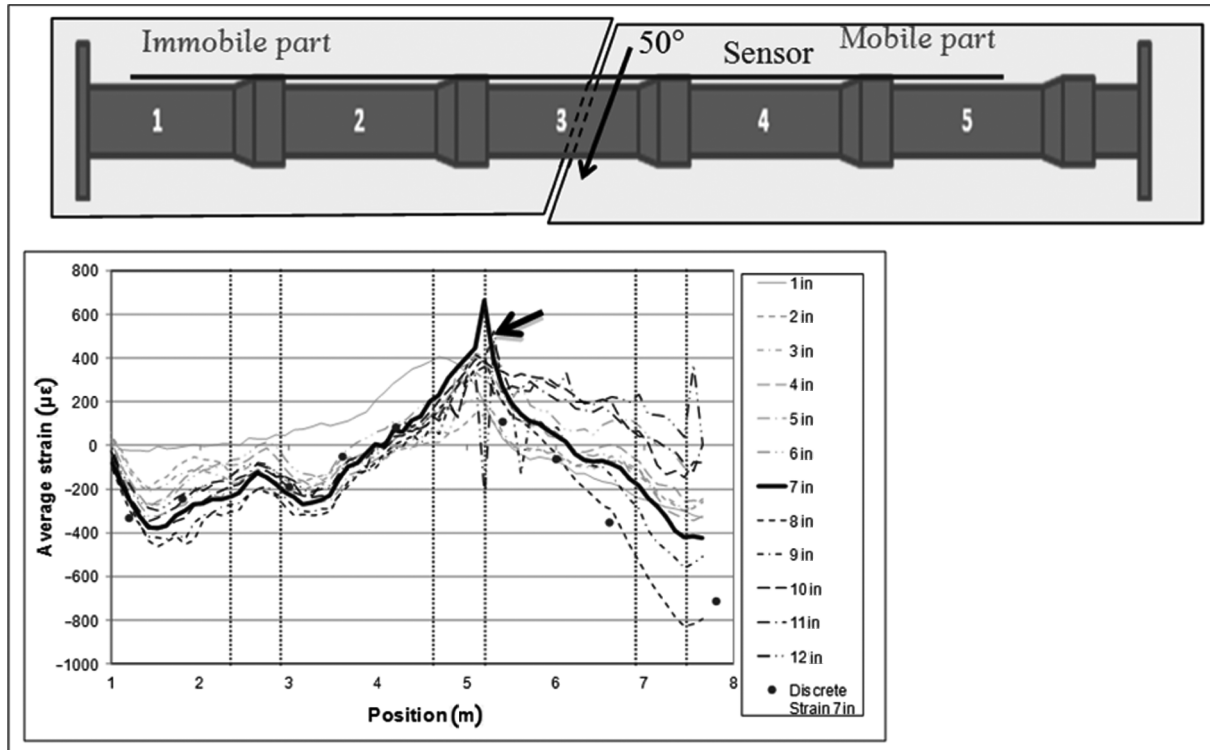


**Figure 16.** Results of test with detected damage (indicated by arrow) in the second test. Strain gauge values: courtesy of Prof. Lynch group at University of Michigan, Ann Arbor, Michigan.

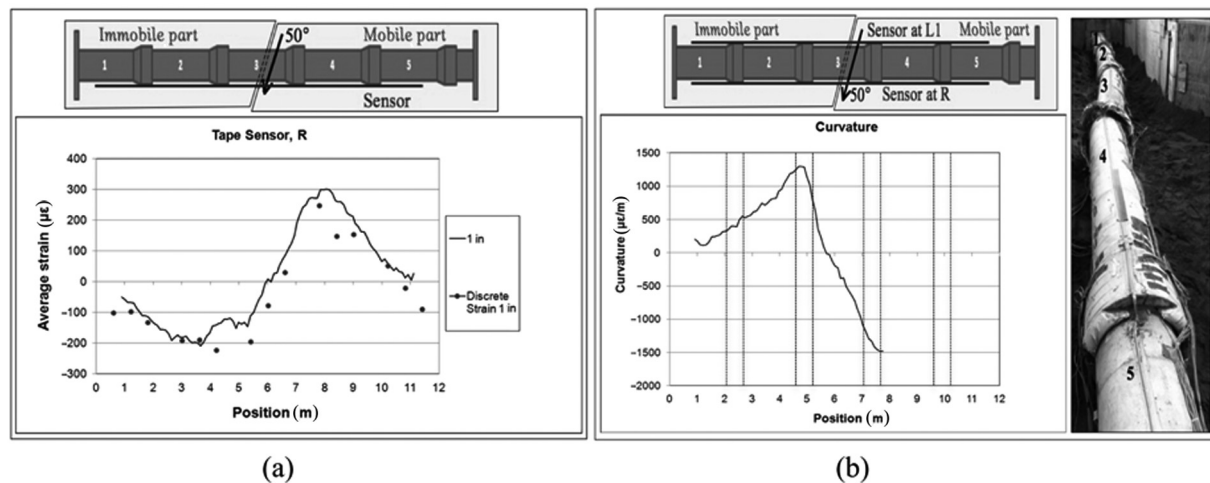


**Figure 17.** (a) Measurement result of Tape sensor at location R and (b) horizontal curvature calculated from measurements of Tape sensors at locations L1 and R and their correlation with the deformed shape of the pipeline. Strain gauge values: courtesy of Prof. Lynch group at University of Michigan, Ann Arbor, Michigan.

- The distribution of horizontal curvature presented in Figure 17 is calculated from strain measurements as a ratio between the difference in strain (strain at L1 minus strain at R) and pipeline diameter; the pipeline body bends so that it has inflection point

(curvature equal to zero) approximately at the shear plane; the curvature is approximately equal to zero at the immobile extremity and approximately linearly changes between the extremity and the joint 2; this indicates that strong concentrated force is

generated at joint 2 due to soil movement; quasi-linear curvature distribution between the joints 2 and 3 leads to similar conclusion at the joint 3.

The ability of the Tape sensors and the parallel topology to assess the deformation of the pipeline was confirmed by the strain gauges and visual inspection of the deformed shape after the excavation of the pipeline. This validates the use of parallel topology for monitoring of deformed shape of the pipeline.

**Analysis of Cord sensor installed at location L1**

Cord sensing cable functioned properly for all 12 increments of the simulated ground displacement in both tests. Cord sensing cable, installed in the form of serpentine (see Figure 5) for the first test, had one part installed on the pipeline at location L1, and the results obtained from this location are presented in Figure 18. The part installed in the soil is presented in section “Analysis of Cord sensor installed in soil at location L3.” As in the case of the Tape sensor measurement, the results were not compensated for temperature.

In order to interpret the measurement of the Cord sensor, it is necessary to understand that the strain measured by optical fiber is not equal to the strain on the structure because the measurement fibers can slide inside the body of the sensor. The sliding of the fibers actually makes interpretation of the data difficult. The fact that one part of the physical sensor was installed on the pipeline and the other part in the soil (the sensor had a shape of serpentine) additionally complicate data analysis since the fibers could slide from one part to the other. Comparison of Cord sensor with strain gauge results was not performed, since the former is less accurate than latter, due to sliding of fibers.

For the applied displacement in range 25.4–203.2 mm (1–8 in), the strain change due to the damage in joints 2 and 3 is visible, but difficult to distinguish from the other strain variations (e.g. due to sliding of the fibers within the tube).

For higher levels of displacement, the damage detection can be performed more reliably, as high strain in diagram (marked by black arrows). However, sliding of the fibers makes impossible to qualitatively evaluate whether damage increased or not (e.g. strain in fibers for 11 in displacement is smaller than the strain for 10 in displacement), and in some cases can completely “mask” the damage (e.g. damage of joint 3 is not identifiable for 12 in displacement, while it was clearly noted for smaller displacements).

Two zones of concentrated high strain are noted at extremities of the pipeline, as shown by gray arrows in Figure 18. There was no visible damage at these locations and the measurement can be explained by both

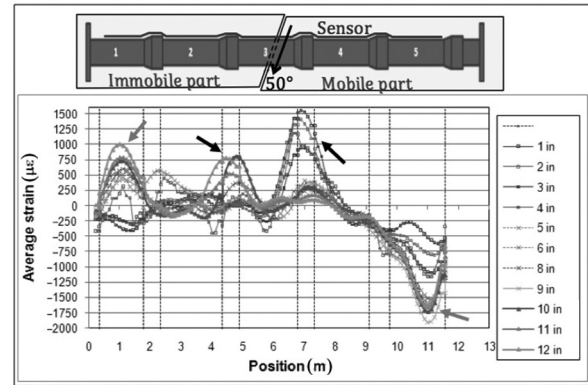


**Figure 18.** Cord sensor measurement at location L1 (on the pipeline) with detected damage (indicated by arrows in black) in the first test.

the influence of real strain change in the pipeline and the sliding of the fibers including the sliding transferred from the parts of sensors embedded in the soil (see Figure 5).

The conclusion carried out from the test is that the Cord sensor can be used to detect and localize the damage; however, only higher levels of the damage can be reliably detected and localized by analyzing time series of the measurement.

**Analysis of Cord sensor installed in soil at location L3**

The Cord sensor embedded in the soil at location L3 (see Figures 5 and 6) successfully detected ground displacement and location of the shear plane, as shown in Figure 19.

Similar to the previous discussion, sliding of the fibers inside the sensor body occurred. In addition, sliding of the sensor with respect to the soil was also possible. Due to both sliding of the fibers and sliding of the entire sensor with respect to the soil, reliable detection and localization of the damage was possible only for higher values of ground displacement and by analyzing the time series of the measurements.

**Analysis of Profile sensor installed in soil at location L2**

The Profile sensor installed in soil at location L2 functioned properly for all 12 increments of the ground displacement in the second test. The measurement results are shown in Figure 20. Profile sensor successfully detected and localized soil displacement as indicated with black arrow in Figure 20. Noise in measurement was observed due to sliding of the sensor within the soil. Stressing of the sensor was detected at the

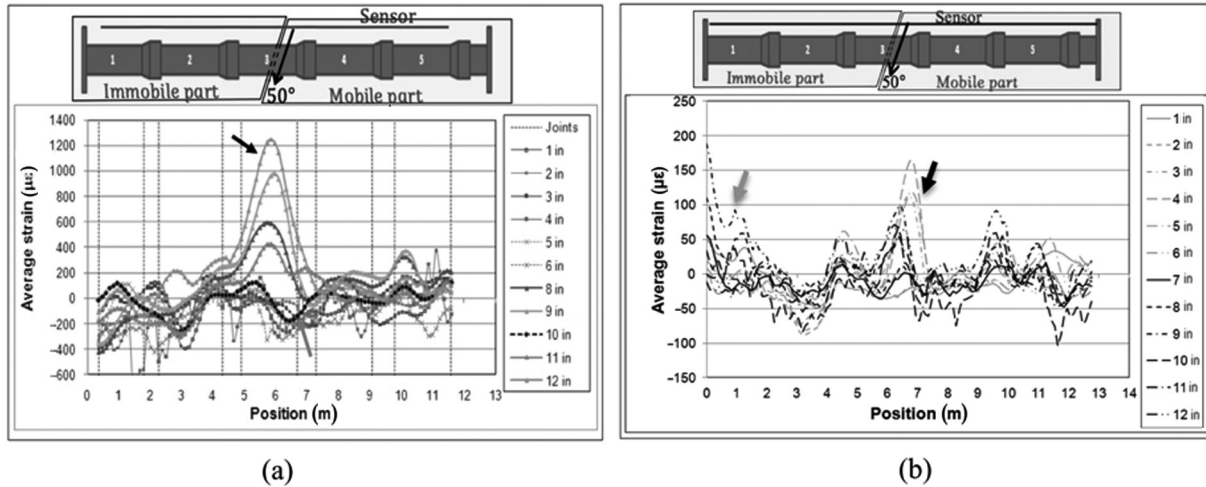


**Figure 19.** Cord sensor measurement at location L3 (in the soil) with detected damage (indicated by arrows in black): (a) first test results and (b) second test results.

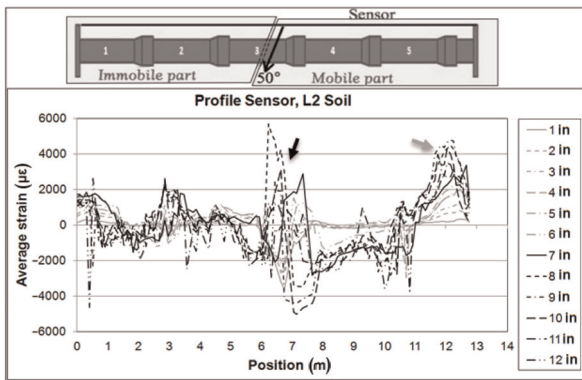


**Figure 20.** Profile sensor measurement at location L2 (in the soil) with detected damage.

extremity of the pipeline due to sharp change in sensor geometry (gray arrow in the figure), for similar reasons as explained for Cord sensor in the first test. While the soil movement can be detected and localized using single measurement of Profile sensor, it is still recommended to confirm the detection and localization by analyzing time series of measurements.

### Statistical data analysis

The data analysis performed in previous subsection was made manually by an experienced engineer. While the engineer's involvement in data analysis should not be removed, it is important to create algorithms for automatic damage detection and localization. The signal produced by damage is at least order of magnitude higher than usual noise (see diagrams in previously presented figures), which makes possible damage detection

and localization using relatively simple threshold algorithms. They can be applied both “in space” (i.e. over the sensed area) and “in time” (i.e. against previous samples). The criteria are summarized as follows:

1. “Unusually high strain variation” at time  $t$  is detected in at least  $m$  neighboring sensing points, where “unusually high strain variation” is defined either by
  - (a) A deterministic threshold (change in value exceed  $d$  microstrain, see example of results in Figure 21 for  $m \geq 5$  and  $d = 150 \mu\epsilon$ ) and/or
  - (b) A simple statistical threshold
    - (i) In time:  $s$  multiples of the standard deviation  $\sigma$  observed over a window of recent measurements (see example of results for  $s = 1, 2, 3$  in Figure 22),
    - (ii) In space:  $s$  multiples of the standard deviation  $\sigma$  observed over a local region of sensors (see example of results for  $s = 1, 2, 3$  in Figure 22), and/or
  - (c) Modified “Z-score” method, which derives statistical thresholds based on the root-squared deviation from the median (i.e. rather than the mean):
 
$$MAD = \text{median}\{|x_i - \tilde{x}|\},$$
 where  $\tilde{x}$  is the sample median;  $M_i = \frac{0.6745(x_i - \tilde{x})}{MAD}$ ; and literature<sup>25</sup> suggests detection when  $|M_i| > 3.5$ .  
 This has shown superior performance in some cases due to its robustness against outliers (see example of results in Figure 23).
2. The strain from at least  $k$  neighboring sensing points reaches value  $p$ , which is associated with



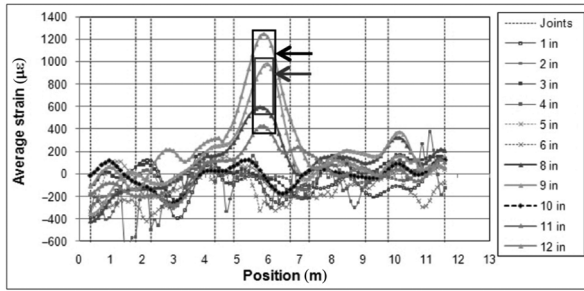


**Figure 21.** Application of deterministic threshold for change in value that exceeds  $150 \mu\epsilon$ , in at least five points; two detections shown between measurements for 203 mm (8 in) and 228.6 mm (9 in) displacement, in gray, and between measurements for 279.4 mm (11 in) and 304.8 mm (12 in) displacement, in black (first test, Cord sensor at location L3).

the ultimate strain limit of the monitored material (see example for  $k = 3$  and  $p = 400 \mu\epsilon$  in Figure 24). This detects slow strain changes that are undetectable by criteria such as those presented in point 1 above. Such degradations are nonetheless important as they can gradually reach critical levels.

In real application, the algorithm parameters ( $m$ ,  $d$ ,  $s$ ,  $M_i$ ,  $k$ , and  $p$ ) should be determined based on measurements performed over nondamaged pipeline during representative (learning) period. Minimal recommended learning period is 1 year in order to identify patterns related to seasonal changes. In the following years, the parameters can be fine-tuned based on measurement results.

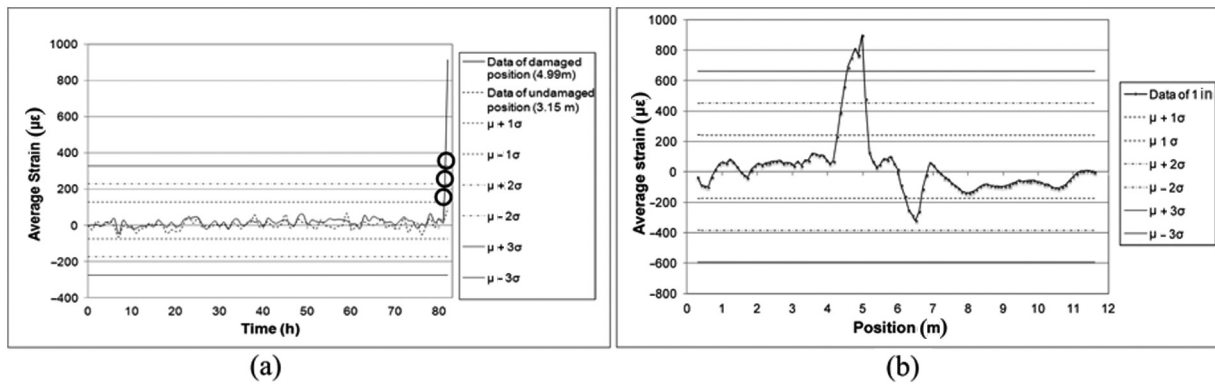


**Figure 22.** (a) Application of statistical threshold “in time”; damage is detected for  $s = 1, 2,$  and  $3$  (see circles); as a comparison, variation of data at nondamaged point does not exceed standard deviation  $\sigma$  (first test, Tape sensor at location L1). (b) Application of statistical threshold “in space”; damage is detected for  $s = 1, 2,$  or  $3$  (see horizontal lines) only at location of damage; variation of data at nondamaged point does exceed standard deviation  $\sigma$  (first test, Tape sensor at location L1).

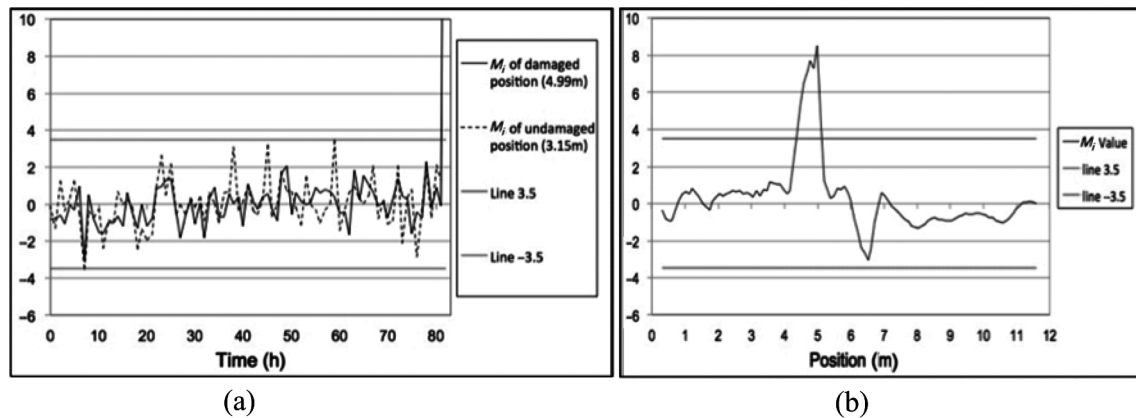


**Figure 23.** Application of Z-score method in (a) time and (b) space to the results shown in Figure 22(a) and (b); the damage is detected at joint 2 but not confirmed in joint 3, indicating that parameter  $M_i$  should be fine-tuned.

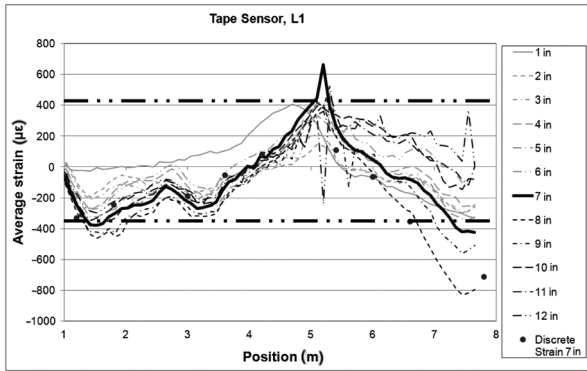


**Figure 24.** Absolute strain threshold damage detection for  $k = 3$  and  $\rho = 400 \mu\epsilon$  (second test, Tape sensor at location L1).

The examples of application of algorithms on the measurement results obtained during the tests are given in Figures 21 to 24. In both tests, the pipeline was monitored continuously for few days before the test, and this period is used as the learning period. Successful damage detection and localization based on algorithms confirm the potential of the method to be fully automated in real applications.

The soil used in both tests had the same properties, thus the sensitivity of algorithms to the soil properties could not be tested. Consequently, to minimize uncertainties, a combination of algorithms is recommended in real-case applications as it can increase the sensitivity to damage and reliability in damage detection.

## Conclusions

The research and development of a novel method for real-time, automatic, or on-demand assessment of health condition of buried pipelines after the earthquake has been successfully accomplished. It included determination of sensor topology, selection and development of sensors, development of installation procedures, implementation, and large-scale testing. The method is based on stimulated Brillouin light scattering in optical fibers and deals with distributed sensors. The following conclusions are carried out from the project:

1. The parallel topology, researched during the project and deployed on the pipeline under the test, is suitable for detection and localization of damage induced by the ground displacement to the concrete segmented pipelines. In addition, the parallel topology applied to sensors embedded in the soil is suitable for detection of ground displacement. Minimum three noncoplanar sensors should be

used for pipeline monitoring and minimum one sensor in the soil, spaced 20–40 cm from the pipeline.

2. Tape and Cord sensors are verified as appropriate for pipeline monitoring, while Profile and Cord sensors are verified for soil monitoring. The sensors installed on the pipeline should be bonded using appropriate adhesives. Peeling demonstrated that the adhesives alternately remained on both pipeline and the sensors, showing no preference of material. To guarantee safe installation of the sensor, the joints of the pipeline should be modified with openings that will accommodate passage of the sensors. The sensors installed in the soil can simply be laid and buried.
3. Two method validation tests were performed to validate the method. Several sensors and several installation procedures were tested. Those that have shown satisfactory performance were adopted and presented in points 1 and 2. Others did not fulfill the requirements, either partially or fully.
4. The data analysis was completed for both validation tests. Manual data analysis was used to achieve the aims of points 1 and 2. Data were compared and validated using results of strain gauges. Algorithms were developed for automation of the method and successfully tested on the results. In the real application, it is recommended to combine algorithms and tune parameters of algorithms based on measurements of nondamaged pipeline over the “learning” period.

The general principles of the method were validated through the method validation testing. The validation tests confirmed the capacity of the method to reliably detect and localize the damage on concrete segmented pipelines and the displacements in the soil. The verification of algorithms confirmed potential for automation. The method deals with parallel topology of distributed sensors that can also be applied to the continuous steel pipelines. The adhesives used in this project can be used for bonding the sensors to steel, based on the authors’ experience and adhesive datasheets. As the joint of steel pipelines are mostly welded, their geometry does not have particular irregularities. Thus, the method developed in this project has potential to be applied to the steel pipelines too.

## Funding

This study is based upon the work supported by the National Science Foundation under Grant No. 0936493 and realized in the frame of George E. Brown Jr Network for Earthquake Engineering Simulation Research (NEESR) Program Solicitation NSF 09-524.

## Acknowledgements

The method validation testing was performed at The Cornell Large-Scale Lifelines Testing Facility, the NEES site at Cornell University (Cornell NEES Site). The authors would like to acknowledge the personnel of the NEES Site and in particular Mr Tim Bond, manager of operations of the Harry E. Bovay Jr Civil Infrastructure Laboratory Complex at Cornell University, and Mr Joe Chipalowski, the manager of Cornell's NEES Equipment Site. This research has been awarded as a payload of NEESR Award CMMI-0724022. The latter hosted this research, and the author would like to thank all the collaborators from the NEESR Award for their precious help and in particular Radoslaw L. Michalowski and Jerome P. Lynch from University of Michigan, Ann Arbor, MI; Russell A. Green from Virginia Tech, Blacksburg, VA; Aaron S. Bradshaw from Merrimack College, North Andover, MA; W. Jason Weiss from Purdue University, West Lafayette, IN; and their students whose help and shared experience significantly contributed to the successful realization of the test. The sensors, the reading unit, and the associated software were provided by SMARTEC SA, Switzerland at significantly reduced costs. Graduate students Dorotea Sigurdardottir from Princeton University and Kai Oberste-Ufer from Ruhr-University Bochum, Germany were involved in and contributed significantly to the success of the validation tests.

## Conflict of interest

Any opinions, findings, and conclusions or recommendations expressed in this material are those of the authors and do not necessarily reflect the views of the National Science Foundation.

## References

1. Torpak S and Taskin F. Estimation of earthquake damage to buried pipelines caused by ground shaking. *Nat hazards* 2007; 40(1): 1–24.
2. Pei Z, Liu Y and Wang X. Earthquake damage assessment models of water supply pipelines and their realization based on GIS. In: *IEEE international proceedings of geoscience and remote sensing symposium, IGARSS '05*, 25–29 July 2005, New York, USA, vol. 7, pp. 5208–5211.
3. O'Rourke TD. An overview of geotechnical and lifeline earthquake engineering. In: Dakoulas P, Yegian M and Holtz RD (eds) *Geotechnical earthquake engineering and soil dynamics III* (GSP No. 75). ASCE, Reston, VA, USA, 1998, vol. 2, pp. 1392–1426.
4. Liu H. *Pipeline engineering*. Boca Raton, FL: Lewis Publishers, 2003.
5. Kobayashi M, Minato H, Kondo M, et al. NKK ultrasonic pipeline inspection pig. *NKK Tech Rev* 1999; 80: 46–50.
6. Sinha SK and Fieguth PW. Segmentation of buried concrete pipe images. *Automat Constr* 2006; 15(1): 47–57.
7. Wirahadikusumah R, Abraham DM, Iseley T, et al. Assessment technologies for sewer system rehabilitation. *Automat Constr* 1998; 7(4): 259–270.
8. Mandayam S, Jahan K and Cleary DB. Ultrasound inspection of wastewater concrete pipelines-signal processing and defect characterization. In: *27th annual review of progress in quantitative nondestructive evaluation, 2001 (Proceedings of AIP Conference, vol. 557)*, Melville, NY, USA: AIP (American Institute of Physics). pp. 1210–1217.
9. Weil GJ. Infrared thermographic pipeline leak detection systems for pipeline rehabilitation programs. *Proc SPIE* 1998; 3398: 54–65.
10. Lynch JP and Hou TC. Conductivity-based strain and damage monitoring of cementitious structural components. *Proc SPIE* 2005; 5765: 419–429.
11. Yoon DJ, Weiss WJ and Shah SP. Assessing corrosion damage in reinforced concrete beams using acoustic emission. *J Eng Mech Div-ASCE* 2000; 126(3): 273–283.
12. Lynch JP, Wang Y, Loh K, et al. Performance monitoring of the Geumdang Bridge using a dense network of high-resolution wireless sensors. *Smart Mater Struct* 2006; 15(6): 1561–1575.
13. Kim J, O'Connor S, Nadukuru S, et al. Behavior of full-scale concrete segmented pipelines under permanent ground displacements. *Proc SPIE* 2010; 7650: 76500U-1–76500U-11.
14. MOI. Case Study – Gas Pipeline. Available at: [www.micronoptics.com/uploads/library/documents/MicronOptics-Williams Pipeline 02008.pdf](http://www.micronoptics.com/uploads/library/documents/MicronOptics-Williams Pipeline 02008.pdf) (2008, accessed 22 June 2012).
15. Inaudi D and Glisic B. Development of distributed strain and temperature sensing cables. In: *17th international conference on optical fiber sensors*, Bruges, Belgium, 23–27 May 2005 (*Proceedings of the SPIE*, vol. 5855), SPIE – The international society for optics and photonics; Bellingham, WA, USA, pp. 222–225.
16. Posey R, Johnson GA and Vohra ST. Strain sensing based on coherent Rayleigh scattering in an optical fibre. *Electron Lett* 2000; 36(20): 1688–1689.
17. Kikuchi K, Naito T and Okoshi T. Measurement of Raman scattering in single-mode optical fiber by optical time-domain reflectometry. *IEEE J Quantum Elect* 1988; 24(10): 1973–1975.
18. Kurashima T, Horiguchi T and Tateda M. Distributed temperature sensing using stimulated Brillouin scattering in optical silica fibers. *Opt Lett* 1990; 15(18): 1038–1040.
19. Nikles M, Thévenaz L and Robert PA. Brillouin gain spectrum characterization in single-mode optical fibers. *J Lightwave Technol* 1997; 15(10): 1842–1851.
20. Thevenaz L, Facchini M, Fellay A, et al. Monitoring of large structure using distributed Brillouin fiber sensing. In: *13th international conference on optical fiber sensors (OFS-13)*, Kyongju, Korea, 12–16 April 1999 (*Proceedings of the SPIE*, vol. 3746) SPIE – The international society for optics and photonics; Bellingham, WA, USA. pp. 345–348.
21. Inaudi D and Glisic B. Long-range pipeline monitoring by distributed fiber optic sensors. *J Press Vess-T ASME* 2010; 132(1): 011701-01–011701-09.

22. Glisic B and Inaudi D. *Fibre optic methods for structural health monitoring*. Chichester: John Wiley & Sons, Inc., 2007 (Europe)/2008 (USA).
23. Glisic B and Inaudi D. Development of method for in-service crack detection based on distributed fiber optic sensors. *Struct Health Monit* 2012; 11(2): 161–171.
24. Ravet F, Briffod F, Glisic B, et al. Submillimeter crack detection with Brillouin-based fiber-optic sensors. *IEEE Sens J* 2009; 9(11): 1391–1396.
25. Iglewicz B and Hoaglin D. *How to detect and handle outliers*. Milwaukee, WI: ASQC Quality Press, 1993.